SHOCK PROPAGATION AND FRACTURE IN 6061-T6 ALUMINUM FROM WAVE PROFILE MEASUREMENTS

By
W. M. Isbell
D. R. Christman

Materials & Structures Laboratory
Manufacturing Development
General Motors Corporation

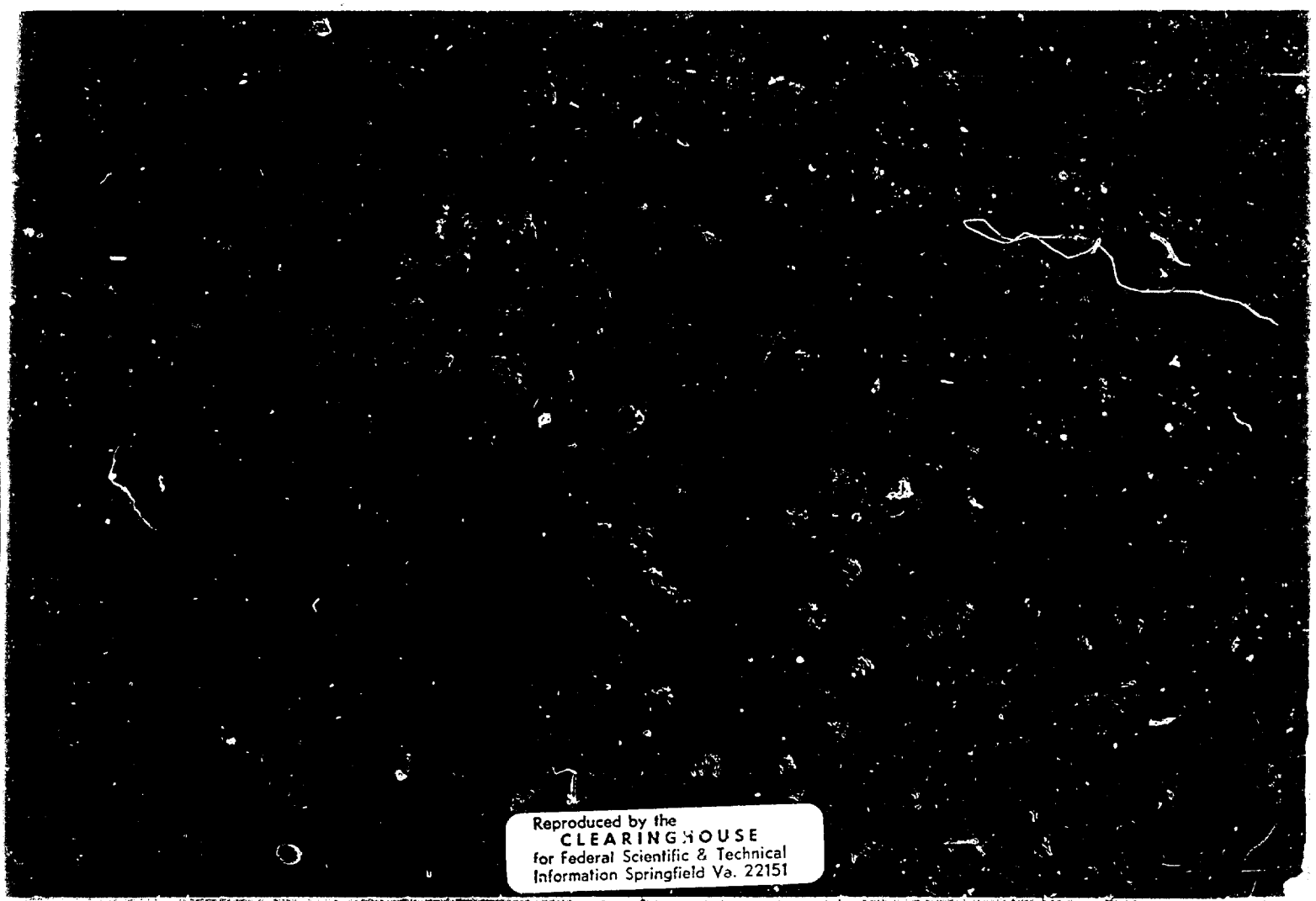

DASA 2419
MSL - 69- 60

COPY No. 19

SHOCK PROPAGATION AND FRACTURE IN 6061-T6 ALUMINUM FROM WAVE PROFILE MEASUREMENTS

This work sponsored by the Defense Atomic Support Agency under NWER/ Subtask AA 106

By
W. M. Isbell
D. R. Christman

Materials & Structures Laboratory
Manufacturing Development
General Motors Corporation

1970, APRIL

Prepared For
Director

Defense Atomic Support Agency
Washington, D.C. 20305
Under Contract DASA 01-68-C-0114

ABSTRACT

The use of high-resolution, time-resolved measurements of rear surface velocity in shock loaded 6061-T6 aluminum is discussed as a means of studying spall fracture. The influence of stress pulse shape, material temperature, maximum compressive stress and degree of fracture on free surface motion is presented and correlated with maximum tensile stress at the spall plane. A summary of dynamic properties data (equation of state, elastic wave velocity, stress-strain-strain rate behavior, spall threshold) and a brief discussion on fracture in metals are also presented.

TABLE OF CONTENTS

LIST OF ILLUSTRATIONS

LIST OF ILLUSTRATIONS (Continued)

INTRODUCTION

The prediction of the response of reentry vehicles to impulsive loading arising from energy deposition has been studied extensively during the last decade. Sophisticated computer routines have been developed to assess the vulnerability of such vehicles to both the initial phase of the loading, in which stress waves are propagated through the structure, and to subsequent phases, where elastic vibration or large permanent deformation may occur.

The present study has been directed towards an examination of the initial phase, where radiation-induced stresses may create transient tensile pulses of such amplitude to induce fracture in the material. The program has provided basic material property measurements required under a larger, DASA sponsored research effort, PREDIX.* Under this program, a large number of dynamic measurements have been made on several classes of materials and the results used as inputs for models of shock wave propagation and fracture dynamics.

This report describes shock wave propagation and spall fracture measurements made on 6061-T6 wrought aluminum alloy. The report concentrates on interpretation of time-resolved, free surface velocity measurements of impacted specimens and use of these measurements as indicators of the complex fracture process occurring within the specimen.

* Work performed under Defense Atomic Support Agency contract DASA-01-68-C-0114.

MATERIAL PROPERTIES

Although this paper is primarily concerned with shock wave propagation and spall fracture in 6061-T6 aluminum, the material has been extensively characterized and representative results are presented here for completeness. 6061-T6 aluminum is a solution-heat-treated and precipitation-hardened alloy (primarily aluminum-magnesium-silicon) and was obtained in the form of rolled sheet with elongation of the grains in the plane of the sheet. All testing was performed with the test direction normal to the plane of the sheet. A summary of mechanical and physical properties of 6061-T6 aluminum is given in Reference 1.

The hugoniot and hydrostat have been determined from uniaxial strain (shock wave) and uniaxial stress tests, the adiabat has been obtained from ultrasonic measurements of elastic wave velocities, and stress-strain-strain rate behavior has been determined from uniaxial stress tests. The stress or pressure vs volume change is given in Figure 1. The hugoniot (σ_H) is based on flat-plate, uniaxial strain experiments up to 200 kbars. The indicated hugoniot elastic limit (σ_H = 6 kbars) is based on measurements of elastic precursor decay and represents the level reached after $\sim$ 5 mm travel. The hydrostat (P_H) was obtained from the hugoniot (σ_H) by subtracting the deviatoric stress component[2]. The adiabat (P_S) was derived from measurements of the pressure dependence (0-10 kbars) of longitudinal and shear wave velocities, results of which are given in Figure 2. The calculated bulk modulus (728 kbar) and its adiabatic pressure derivative (4.6) were used to predict the dependence of volume on pressure[3]. The calculated hydrostat and adiabat agree to within 1% up to 200 kbar.

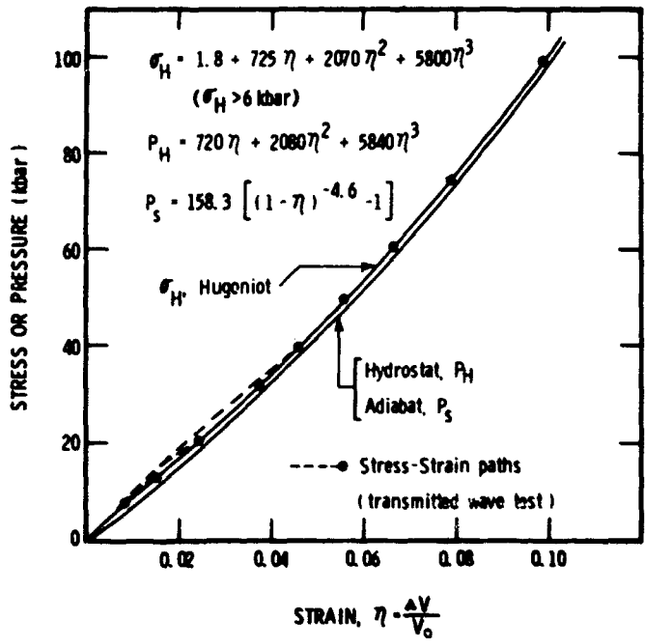

Figure 1 Stress-Volume Equation of State for 6061-T6 Aluminum at 25°C

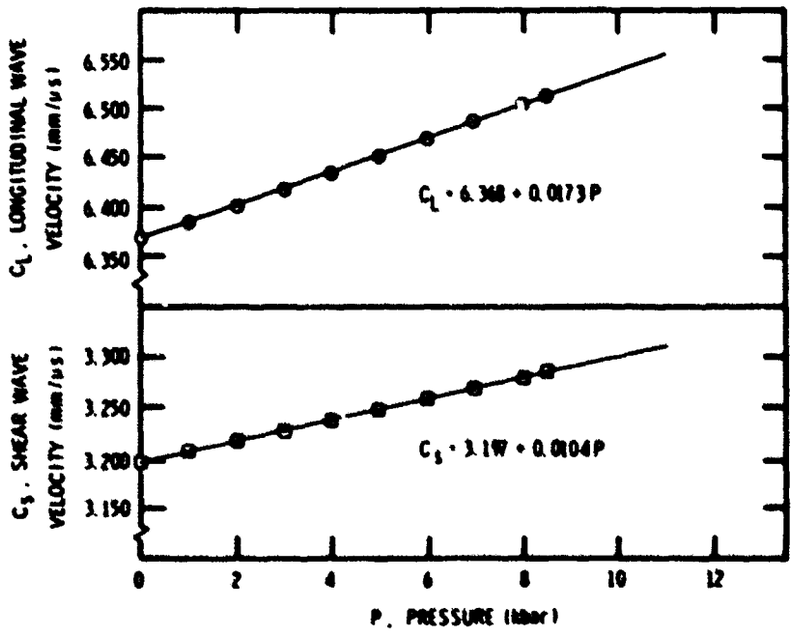

Figure 2 Elastic Wave Velocities for 6061-T6 Aluminum at 25°C, Including Pressure Dependence (Isothermal)

The uniaxial stress-strain-strain rate behavior of 6061-T6 aluminum is shown in Figure 3[4]. The rate sensitivity is very low at room temperature (25°C) for strain rates up to 10^3/sec, but becomes appreciable at 288°C, showing an increase of about 50% in yield for an increase in strain rate of over 5 orders of magnitude. Observations of fracture surfaces for strain rates from quasi-static up to that found in spall tests have shown that material failure is of a ductile nature[5].

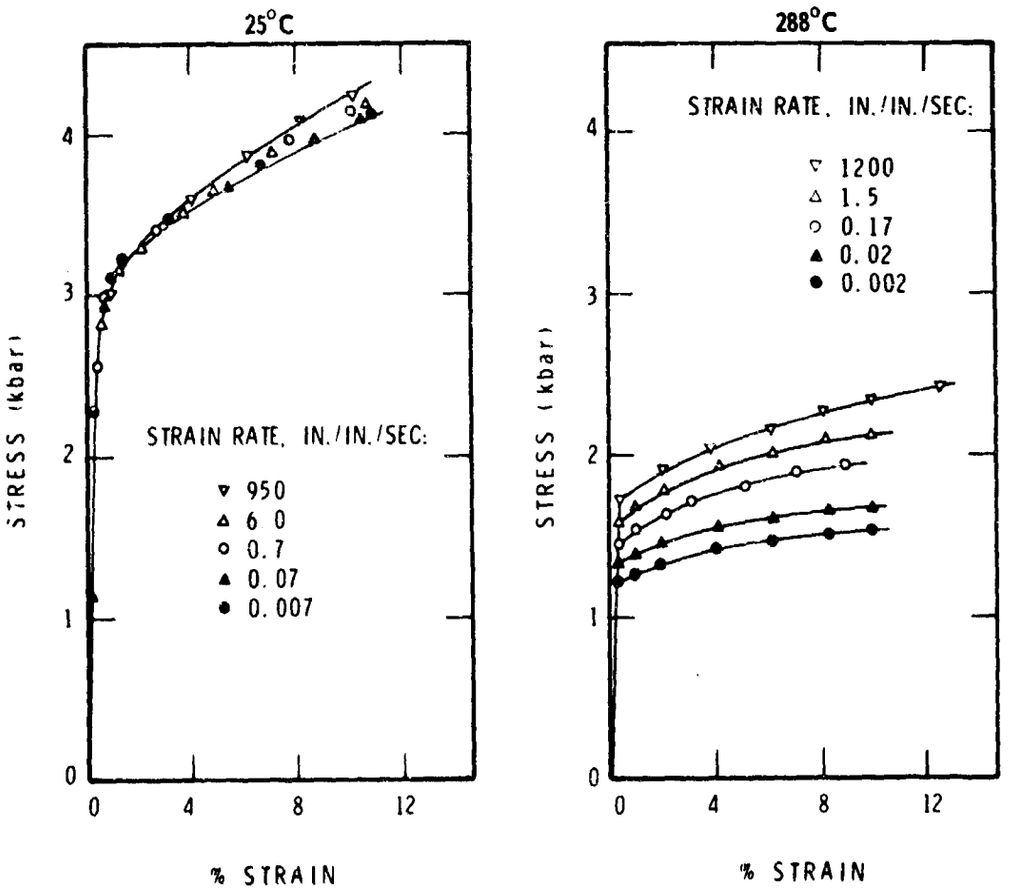

Figure 3 Stress-Strain-Strain Rate Behavior for 6061-T6 Aluminum in Compression

FRACTURE

Fracture in metals can be considered to be of two types: brittle or ductile. The type of fracture is related to the physical and mechanical properties of the material, but is also influenced by test temperature and loading history and rate. When a metal is subjected to sufficient stress, then slip, twinning or cleavage may occur, depending on which mode has its critical value exceeded first by the resolved stress. For a given metal, the relative values of these stresses can change appreciably, particularly as a function of temperature and crystal or grain orientation relative to applied stress.

Brittle fracture is characterized by transgranular cleavage and often occurs in HCP and BCC structures, but usually not in FCC metals. Crack nucleation in brittle fracture is associated with some degree of plastic deformation, which may be slip on a microscopic scale as dislocations move to form pile-ups or may be deformation twinning. Dislocation pile-ups can lead to stress concentrations large enough to initiate cavities or microvoids at grain boundaries, slip bands, twins or other such obstacles. These microcracks can coalesce and propagate under the action of an applied stress, provided the elastic strain energy is not dissipated by plastic flow.

Ductile fracture is usually characterized by nucleation, growth and coalescence of voids or holes, giving a fibrous surface consisting of relatively smooth, concave depressions[6]. Voids often originate at stress concentrations resulting from dislocation motion and pile-up at grain boundaries or imperfections, or in regions of heavy plastic deformation. Subsequent growth and coalescence of these voids is accompanied by a large amount of plastic flow. Uniform plastic strain in

the direction of the applied stress gives normal rupture where the resulting depressions are essentially circular. Shear rupture occurs under the combined effects of plastic strain in the applied stress direction and shear strain in the maximum shear stress plane. Tearing is the result of non-uniform strain in the applied stress direction. Both shearing and tearing result in elongated or parabolic dimples on fracture surfaces.

SPALLATION

The tensile stress condition usually associated with spall fracture results from reflection of compressive stress pulses from a relatively low impedance interface (usually a free surface) and their subsequent interaction. Analysis of spall fracture in metals requires consideration of a number of factors, most important of which are material properties, stress-time history and test technique. This section is concerned with test techniques and some representative results.

There are a number of methods of generating stress or shock waves of sufficient magnitude to create spall fractures in a material, including gun-launched flat plates[7], electrically or magnetically accelerated flyer plates[8], explosive loading[9], and x-ray or electron beam deposition[10]. The gun-launched, flat-plate technique was used in conducting the shock wave and fracture studies described in this paper. This method gives close control over stress-time history of the input pulse, permits change in the shape of the spall-producing tensile pulse, is compatible with the use of high-resolution diagnostic techniques, and permits easy recovery of test specimens.

The spall behavior of a material is generally studied by carrying out a series of impact and recovery tests, where the target specimen is then sectioned across a diameter, polished, etched and examined optically at a magnification of 50 to 100X. The specimen is then graded or classified according to the degree of fracture that has occured, which can range from no observable fractures to complete material separation. The incipient spall threshold is defined as the impact velocity (for a given set of test parameters) corresponding to the onset of microfracture. Occasionally, a few microcracks may appear at lower velocities, but these appear to originate at material flaws where conditions for fracture initiation are not representative of bulk material properties. Therefore, the incipient threshold is based on cracking over approximately 50% of the specimen (on a projected length basis). One could also establish a complete fracture or separation threshold, but this is not recommended as a primary spall criterion since it is more likely to be influenced by edge effects (loss of one-dimensional strain conditions) and by recovery-induced damage.

The nature of spall fractures in ductile and brittle metals is shown in Figures 4 and 5. In Figure 4, tantalum shows a classic form of ductile failure, i.e., formation of almost perfectly spherical voids, while beryllium shows cleavage cracks typical of brittle failure. The aluminum alloy has also failed in a ductile manner, although the appearance of the fractures is quite different from tantalum, possibly due to the elongated structure and secondary constituents in the aluminum alloy. The scanning electron microscope (SEM) pictures in Figure 5 (looking at the half surface of a completely separated specimen) further illustrate differences between ductile and brittle fracture.

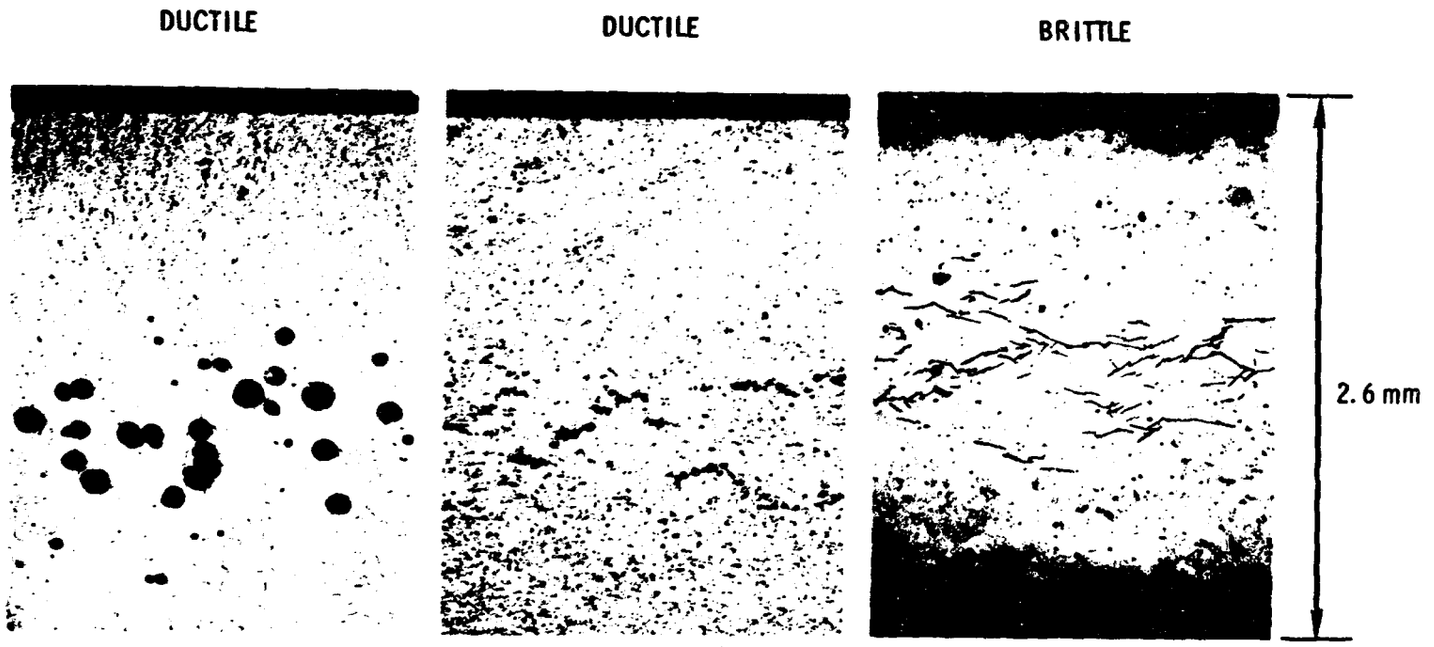

Figure 4 Spall Fractures in Ductile and Brittle Materials, Optical Micrographs

Figure 5 Surfaces Created by Spall Fracture in Ductile and Brittle Materials, Scanning Electron Micrographs

Spall fracture characteristics of 6061-T6 aluminum are shown in Figures 6, 7 and 8. It can be seen in Figure 6 that for a given material and test geometry, spall cannot be defined in terms of a unique impact velocity or stress, but requires consideration of the degree of fracture. This leads to a velocity range over which spall progresses from isolated cracks or voids only a few grains in size to complete material separation across the entire spall plane. The voids may be initiated as the result of dislocation pile-ups at brittle particles (precipitates or inclusions) causing stress concentrations at the particle-matrix interface which lead to void formation and fracture[11]. The onset of fracture is generally referred to as incipient spall and is a critical point since it can be used as a measure of the dynamic fracture strength, and corresponds to generation of sufficient free surfaces within the material to reflect a portion of the interacting tensile pulse as a compressive wave. Figure 7 shows the nature of incipient spall fractures in 6061-T6 aluminum plate. The direction of stress wave propagation was vertical. Note that the fractures follow the direction of grain elongation although there is a tendency for cracks to link up at right angles to this direction. The peak compressive uniaxial strain was about 2% and deformation bands are prominent in some of the grains. SEM pictures of fracture surfaces are shown in Figure 8. Note that failure has been primarily by normal rupture, with evidence of shearing near the necked or peripheral areas. Small particles visible in the depressions in the high magnification (right-hand) picture may be brittle particles that have become exposed during void growth.

Figure 6 Spall Fractures in 6061-T6 Aluminum at 25°C, Optical Micrographs

MSL-69-60

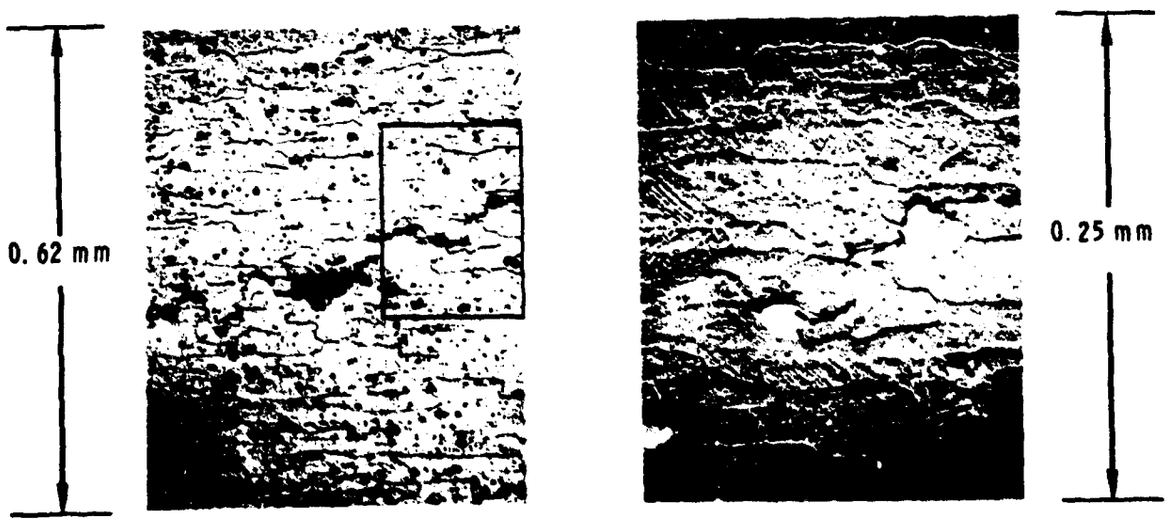

Figure 7 Incipient Spall in 6061-T6 Aluminum at 25°C, Optical Micrographs

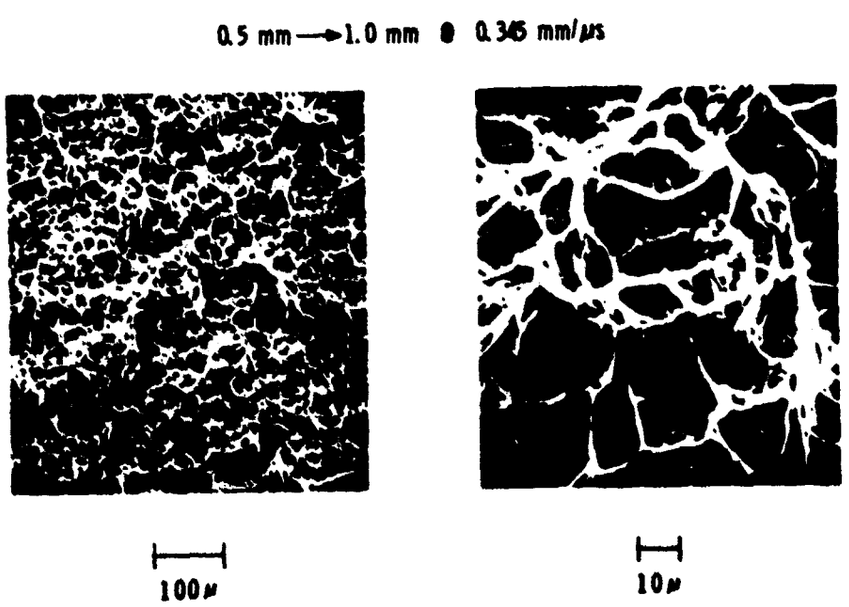

Figure 8 Spall Fracture Surface in 6061-T6 Aluminum, Scanning Electron Micrographs

The "time dependence" of spallation is shown in Figure 9 for 6061-T6 aluminum sheet. Although data are presented in terms of impact velocity vs impactor thickness for nominally rectangular pulses, the results indicate that the onset of fracture is a function of stress-time history, since impact velocity and impactor thickness are proportional to stress and time of loading, respectively. This relationship has been studied by a number of investigators and there is not yet agreement on either a physical description of the fracture process or its dependence on factors such as precompression, stress rate, stress gradient, or tensile pulse magnitude and width[12-16].

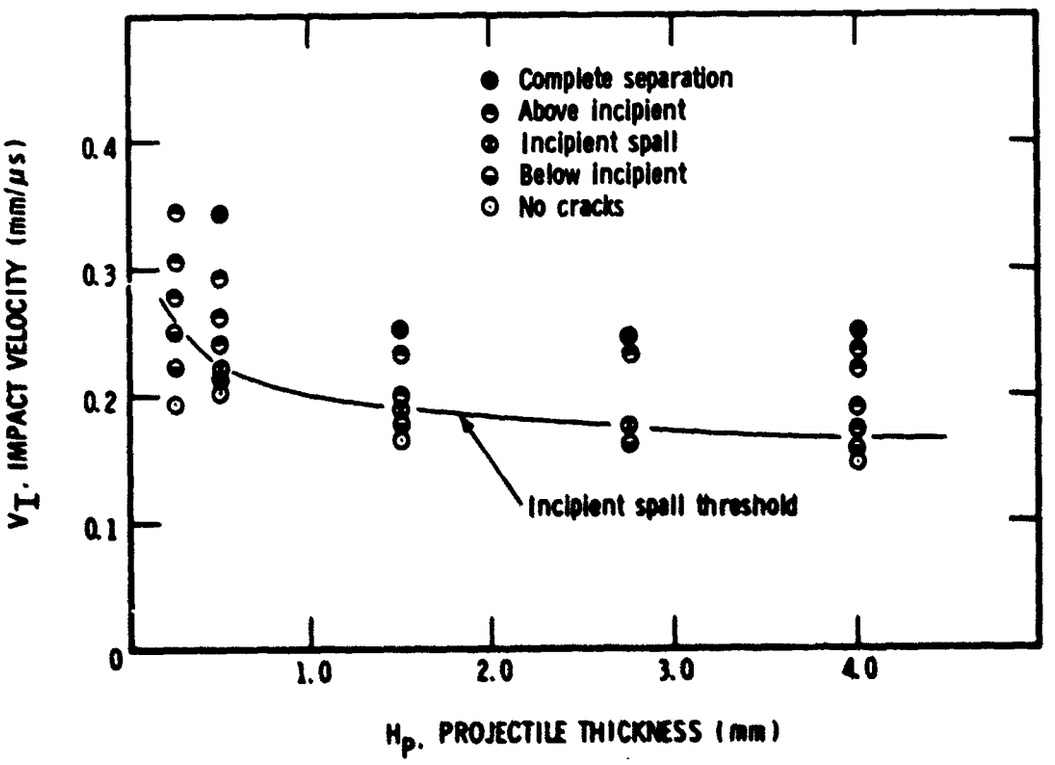

Figure 9 Spall Behavior in 6061-T6 Aluminum at 25°C

Although passive spall tests (i.e., recovery tests) and graphical presentation of data permit one to establish spall thresholds for a material, they do not provide a convenient method of deducing stress-time history associated with a given test. This requires use of active diagnostic instrumentation to measure wave profiles under spall producing conditions. Results of such measurements are presented and discussed below, and are intended to provide quantitative data on mechanisms of spall fracture.

WAVE PROFILE MEASUREMENTS

Due to the difficulty of making high resolution measurements of wave profiles within a shocked specimen, experimenters have utilized time-resolved velocity measurements of the specimen rear surface as an indicator of the behavior of the compressive and release wave systems[17,18]. Interpretation of free surface velocity measurements, however, is complicated by the necessity of predicting wave behavior within the material at a spall "plane", which is actually a volume of material in which time-dependent fracture occurs. To properly reconstruct the wave profile, and wave interactions, it is necessary to assume a model of the material behavior. Measurements made under varying impact conditions are used to assess the accuracy of the model.

A schematic of the experimental system used in the wave profile tests is shown in Figure 10. A flat disc is launched by a 100 mm bore diameter compressed gas gun, by a 65 mm single-stage powder gun, or by a 65 mm two-stage light gas gun. The disc is caused to impact an instrumented specimen with the

velocity controlled to ±1%. An array of electrically charged pins placed around the specimen is used to measure impact velocity and planarity of impact (tilt) as well as to start instruments used to measure shock wave parameters. Standard techniques are used in specimen design to assure a state of one dimensional strain during the time of observation. Figure 11 shows typical components: a sabot with impactor and a target (rear view) with a fused quartz "window" for use with a laser interferometer.

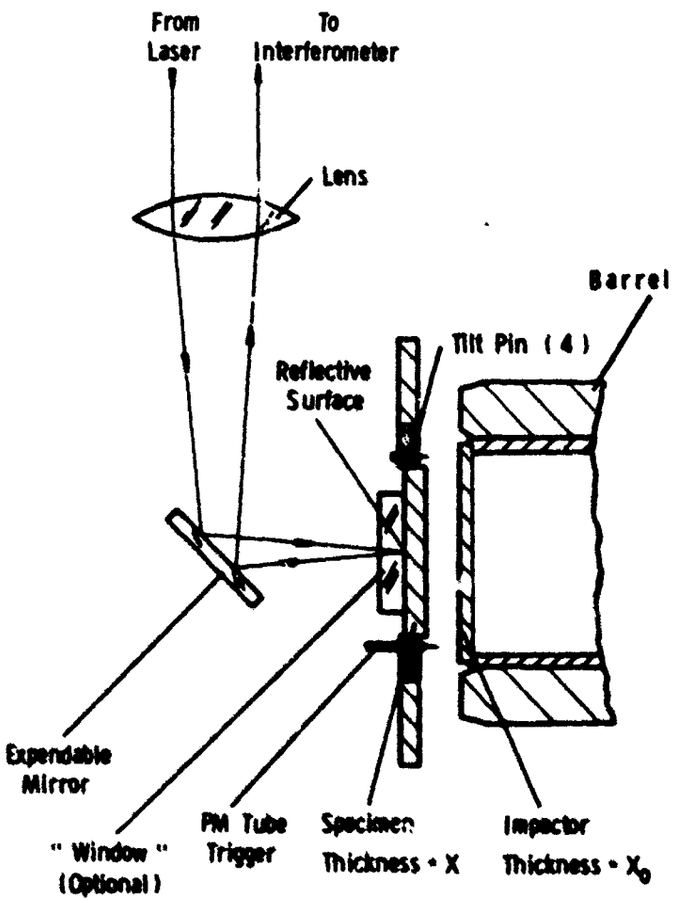

Figure 10 Schematic of Experimental System for Wave Profile Measurements with a Laser Velocity Interferometer

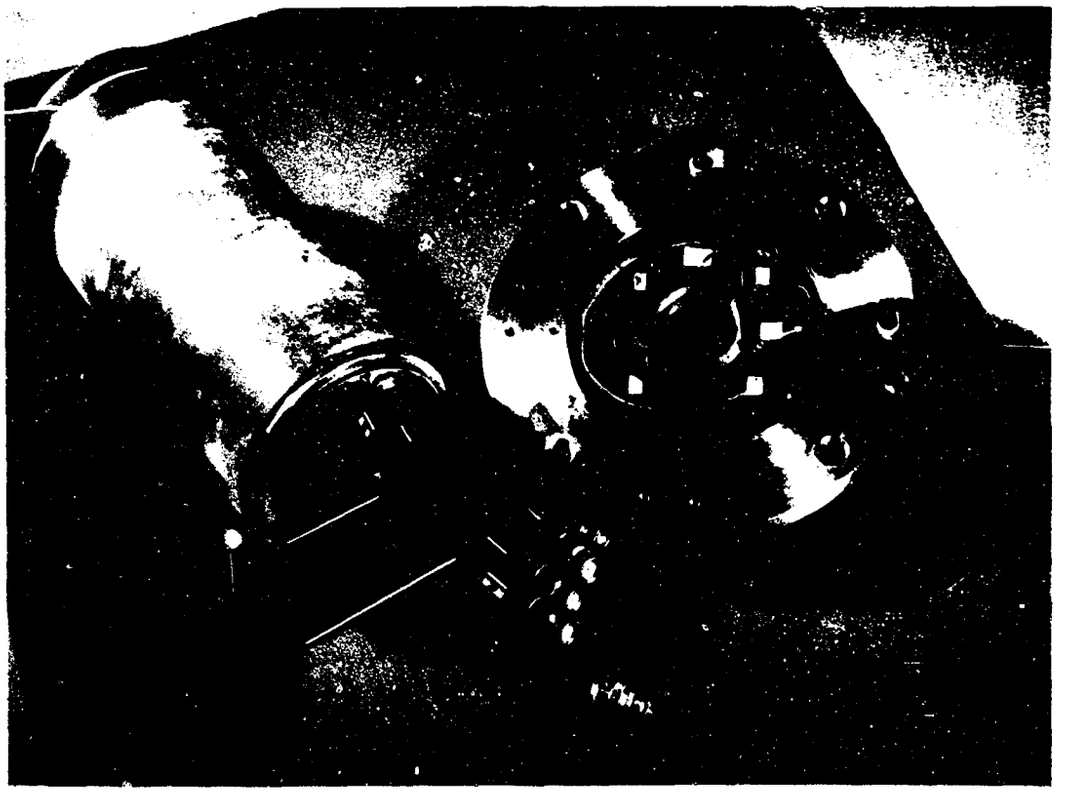

Figure 11 Photograph of Target and Impactor Assembly Showing a Copper Target with Fused Quartz "Window" and an Aluminized Fused Quartz Impactor Mounted in a Sabot

The laser velocity interferometer used to measure motion of the rear surface of a shocked specimen has been discussed by Barker[18]. A single-phase gas laser is focused on the rear surface of the specimen and the reflected beam is directed through an interferometer system which responds to changes in surface velocity as changes in the fringe pattern focused on a fast-response photomultiplier tube. The photomultiplier output is recorded on oscillograms and analyzed to give the velocity-time history of surface motion. The interferometer is shown with the 100 mm compressed gas gun in Figure 12.

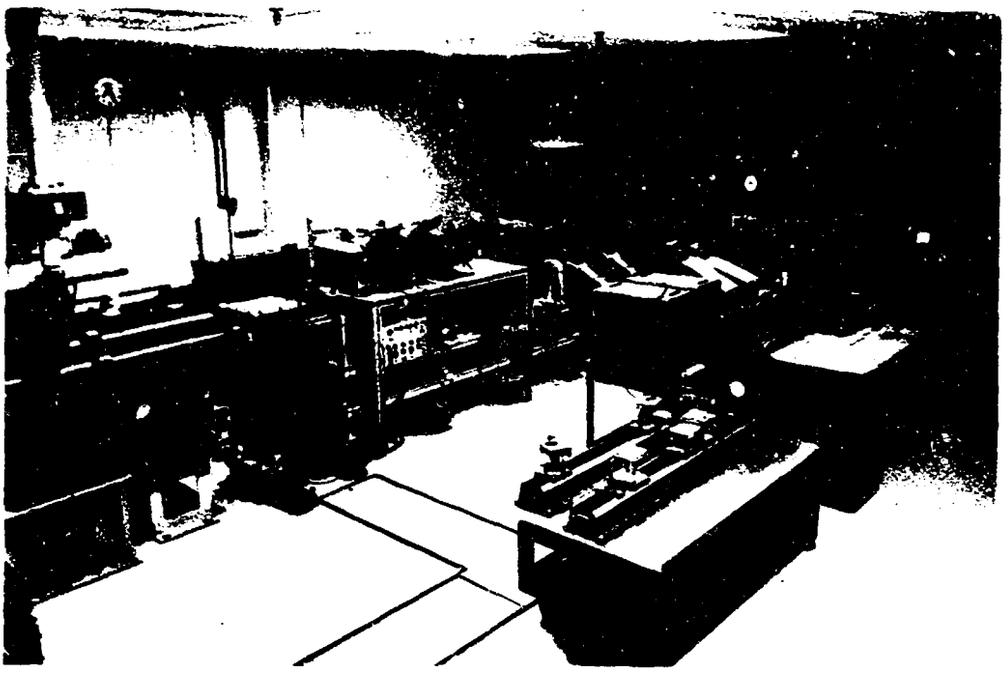

Figure 12 Laser Interferometer Shown Installed on 100 mm Bore Diameter Compressed Gas Gun

For tests in which it is desired to reduce spall-producing reflections, a transparent material of similar impedance to the specimen is bonded to the rear surface and the interferometer is focused on the specimen surface through the transparent "window". Changes in optical path length due to the change in index of refraction of the window material as it is traversed by the shock wave are incorporated into the analysis.

The interferometer system is capable of extremely high time and spacial resolution (2-5 nsec and 0.2 microns) and measurements using this system are relatively insensitive to

shock wave tilt, the nemesis of manganin wire, x-cut quartz, variable capacitor, and other systems used to measure wave profiles. Data are obtainable up to stresses where the surface reflectivity is seriously degraded by the action of the shock wave (100-200 kbars for many materials).

Wave interactions from an impactor striking a specimen of similar material are shown in Figure 13. Several simplifying assumptions are made. The shock is shown as a single wave rather than an elastic-plastic wave system, and the release waves originating at boundaries are considered simple, centered rarefaction fans. Also, small interactions between shock waves have been omitted. Fracture of the material is assumed to occur along a single surface (spall plane) rather than in a volume around this plane (see Figure 4). Wave interactions at the spall plane are shown as if the material exhibits a time dependent fracture, i.e., the percentage of

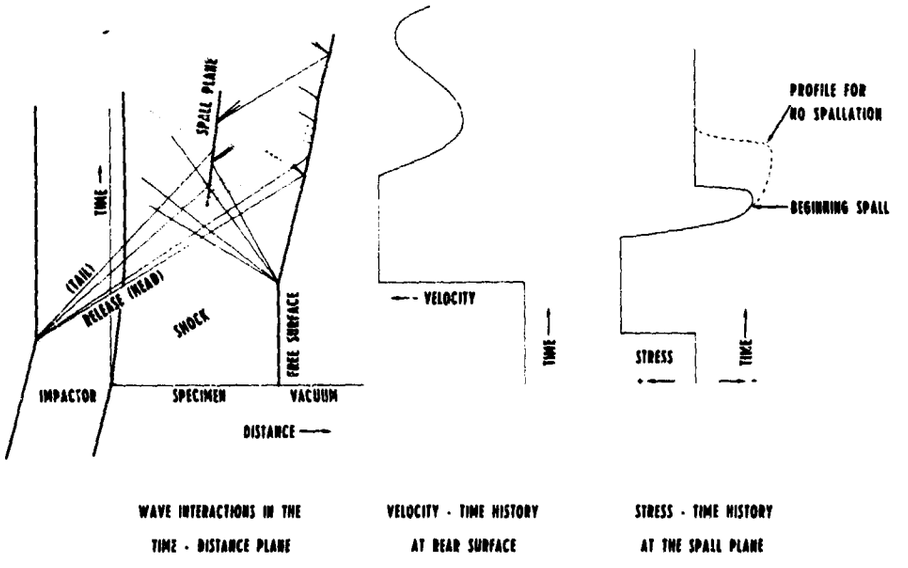

Figure 13 Wave Interactions in Spall Test and Resultant Velocity and Stress History

fractured area in the spall plane increases with time until the entire spall surface has separated. During the early stages of the fracture process, before complete separation is achieved, waves crossing the spall plane are partially transmitted and partially reflected. After complete separation has occurred, any waves trapped in the spalled piece reverberate, giving a decaying, sinusoidal motion to the rear surface as the wave is damped by viscous forces. The magnitude of the exponential decay constant may be related to dislocation processes as described by Taylor[17].

Details of the free surface motion of an aluminum impactor striking an aluminum target are shown in Figure 14. For this test, the specimen was heated to 153°C over a period of ten minutes. An elastic wave of approximately 6 kbars preceeds the plastic wave. A reverberation of this elastic wave between the free surface and the plastic wave can be seen as a small perturbation on the front of the plastic wave. The plastic wave ramps towards a final velocity which remains constant until rarefactions originating from the free rear surface of the impactor arrive and decrease the velocity of the surface. For tests in which no spall occurs, the decrease continues until the velocity is returned nearly to zero.

Evidence of fracture in and about the spall plane is shown in the reversal in the velocity of the surface at approximately 0.7 microseconds. Signals from fractured surfaces reach the rear surface with components of velocity opposite in sign to the rarefaction waves. As the fracturing progresses, the surface is no longer "pulled back" by the release wave system, and accelerates, only to be decelerated again as the entrapped wave reverberates back and forth between the spall surface and the specimen rear surface. If it is assumed that the decrease

of the free surface velocity to the point of reversal (referred to as "pullback") is related to the maximum tensile stress at the spall plane, a quantitative measure of the negative stress required to fracture the material for a given waveshape is provided by the profile. The functional form of the relationship between the maximum tensile stress and pullback has not been firmly established, but attempts to correlate experimental results with calculations of spall plane stress have resulted in the following[17,19].

$$\sigma_t = \rho C \frac{\Delta V}{2} \qquad (1)$$

where σ_t is maximum tensile stress at the spall plane, ρ and C are local density and longitudinal velocity, and ΔV is pullback.

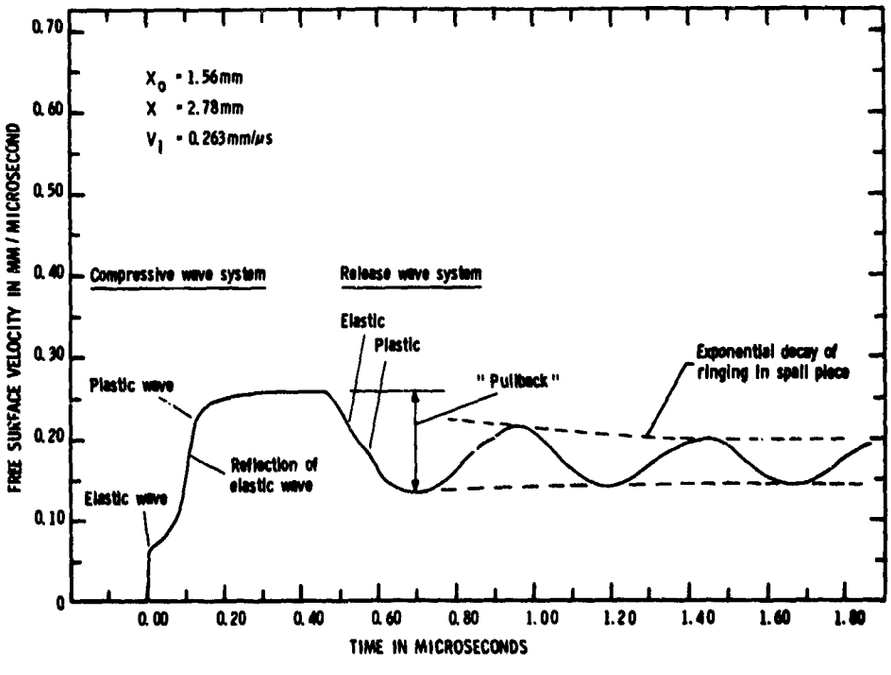

Figure 14 Free Surface Velocity Profile of 6061-T6 Aluminum at 153°C

It should be noted that the calculations that have been compared with Equation 1 are subject to some uncertainties, particularly with regard to the negative pressure equation of state, the fracture mechanism, and the loss of uniaxial strain conditions in the spall plane.

The pullback has been found to be relatively insensitive to the maximum compressive stress as well as to the degree of fracture at the spall plane, for a given impactor thickness. Pullback data corresponding to impact stresses of 15 to 40 kbars are shown in Figure 15. (The results in both Figures 15

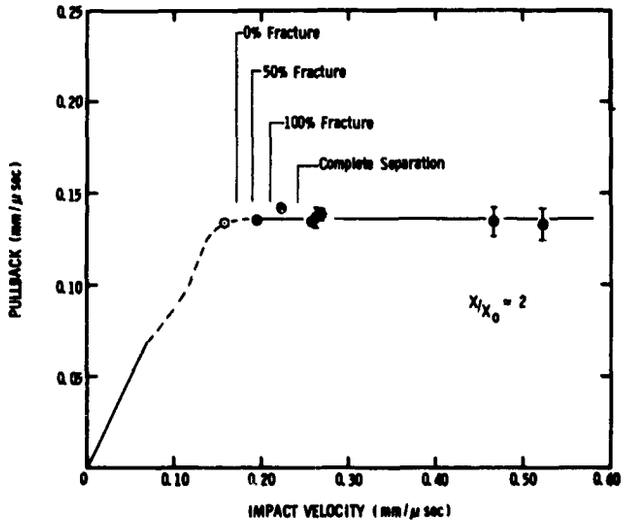

Figure 15 Relation of Pullback to Impact Velocity and Degree of Fracture (Percent Fracture Refers to Fraction of Area Exhibiting Cracks on a Projected Length Basis)

and 16 are for 1.5 mm impactors). In the elastic range, pullback equals impact velocity, while at impact velocities causing fracture, the pullback is approximately 0.135 mm/μsec. (independent of degree of fracture and maximum stress), corresponding to 12 kbars (Equation 1). Thus, the pullback appears to be associated with the incipient spall threshold, i.e., the formation and initial coalescence of voids in the

material, rather than with complete fracture or separation. This useful conclusion may allow comparison of the dynamic fracture strength of the material over a range of wave shapes and times of loading without the necessity of conducting all tests with exactly the same degree of final fracture. An additional benefit may result if the pullback can be related to the results of the recovery-type measurements of the incipient spall threshold. Then a single wave profile test could, for a given set of initial conditions, provide the same incipient threshold data as a series of recovery tests.

A correlation between wave profiles and degree of fracture can be seen in Figure 16. The four tests range from below the impact velocity needed for incipient spall (bottom trace) to above the threshold for complete separation (top trace). The impact velocities relative to the spall thresholds are shown in the center column and refer to velocity scales on the respective profiles. Photomicrographs of recovered specimens are shown to indicate the degree of final fracture. In these and subsequent pictures, the specimen rear surface is shown at the top. Although pullbacks are essentially the same for different degrees of fracture, the amplitude of "ringing" in the spall piece decreases with decreasing damage. For a lesser degree of fracture, less of the wave is trapped in the spall piece, due either to differences in the areas of fractured material at the spall planes, or to differences in the rates at which cracks grow. Thus the degree of fracture can be qualitatively assessed from the amplitude of ringing in the spall piece.

The dependence of spall threshold on time of loading, noted in the recovery experiments described earlier (Figure 9), may be seen in the wave profiles shown in Figure 17. Impactors

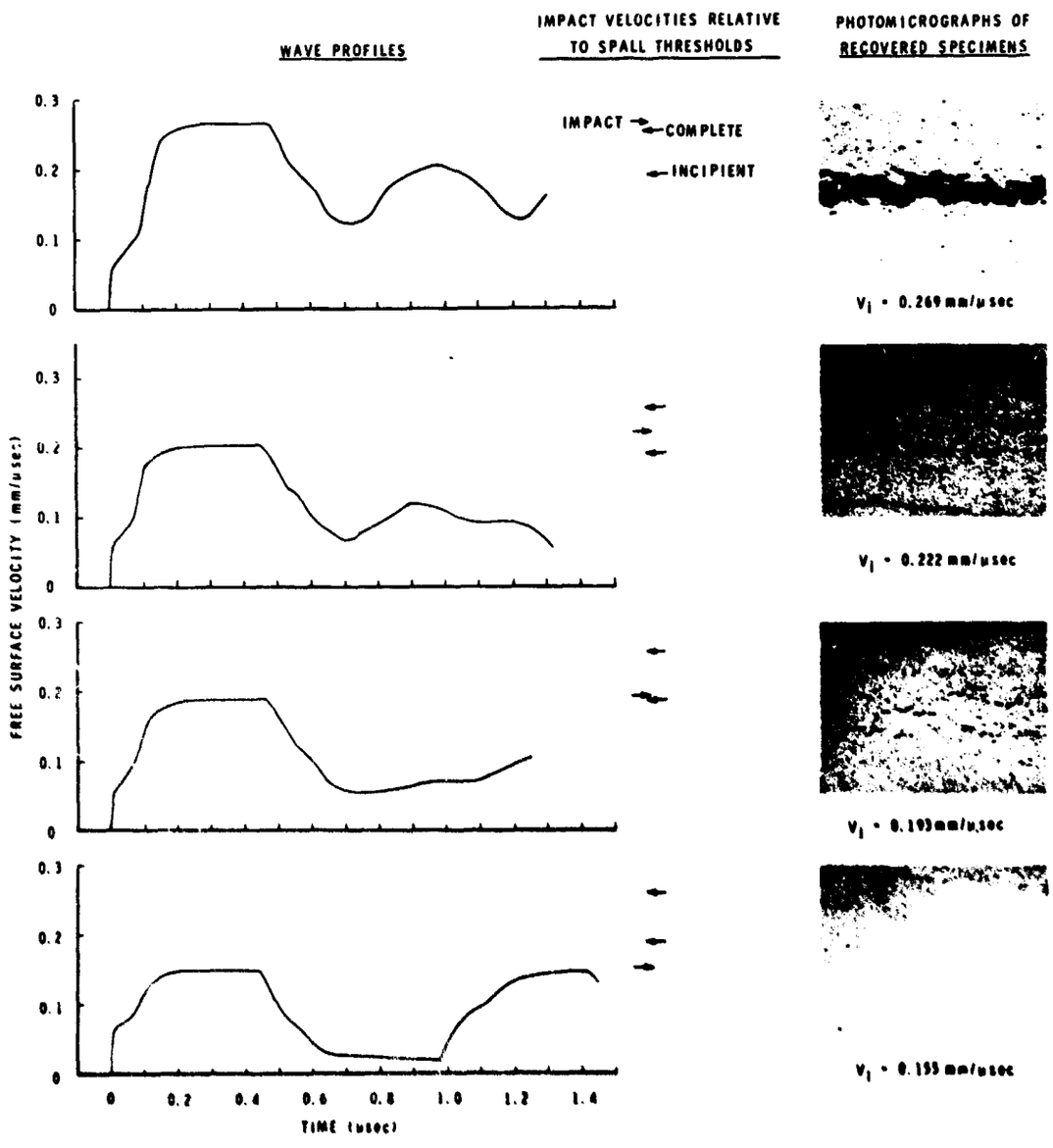

Figure 16 Wave Profiles for Spallation Tests Conducted at Velocities Near the Thresholds for Incipient and Complete Spall

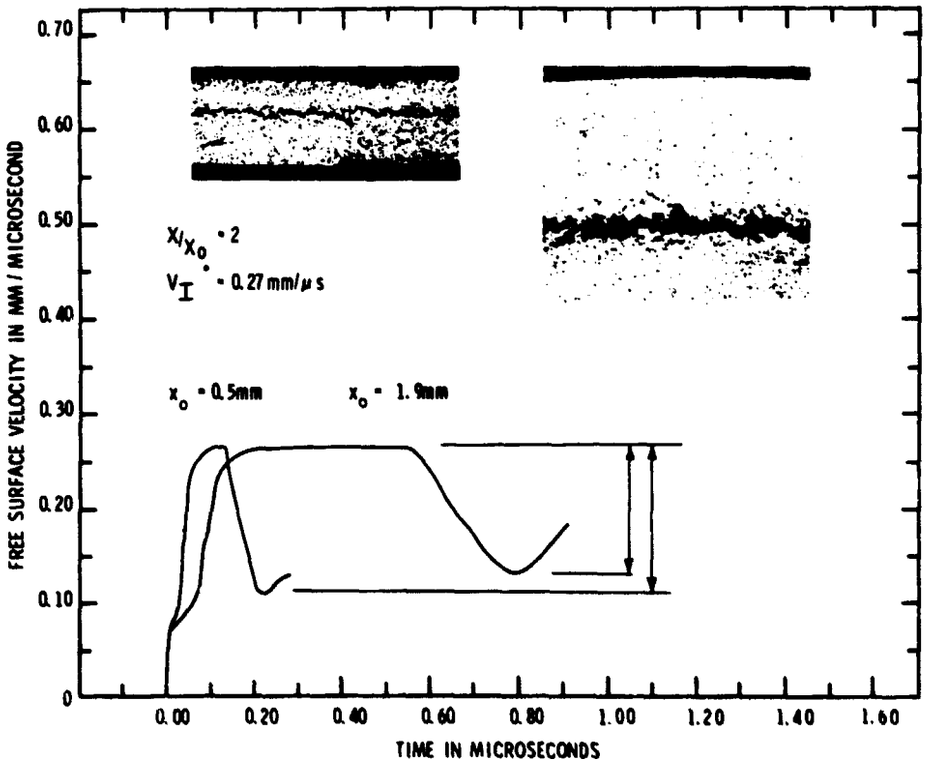

Figure 17 Spall Profiles at Two Times of Loading

0.5 mm and 1.9 mm thick were fired at targets twice as thick at velocities above the threshold for complete spall. The pullback on the test with a shorter time of loading is 18% greater than for the longer time, and corresponds to a maximum tensile stress of 14 kbars.

The behavior of wave profiles as a function of peak stress is shown in Figure 18 for three tests conducted at 21, 35, and 40 kbars. The change in the time for reversal and in the initial (positive) slope of the rebound at higher stresses is probably an indicator of the rapidity with which the spall surface formed. The higher stress gradients s n in the wave fronts of higher velocity tests could also contribute to these changes.

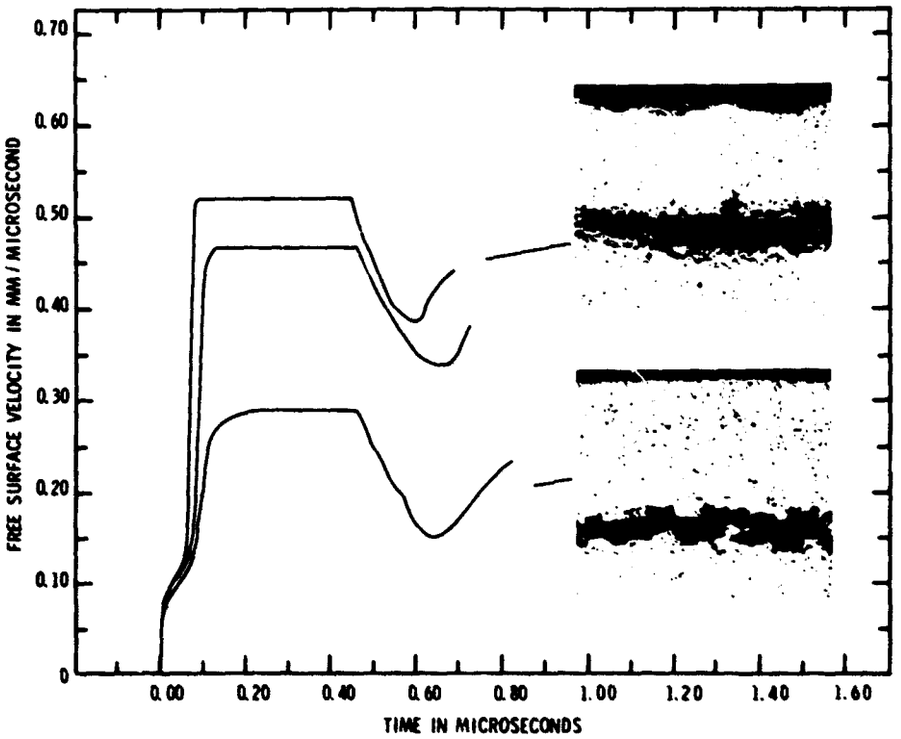

Figure 18 Behavior of Spall Signal for Three Impact Stresses Above the Spall Threshold

The influence of spall plane strength was studied with a target having an "artifical" spall plane of essentially zero strength. This zero-strength plane was actually the interface between two target plates bonded together with a thin (<0.003 mm) epoxy layer having a tensile strength of ∿ 0.01 kbars. The rear target plate was the same thickness as the impactor, putting the interface at the nominal spall plane. Referring to Figure 19, for a single wave system with negligible increase in entropy the free surface velocity would be expected to increase abruptly to the impact velocity. The momentum of the

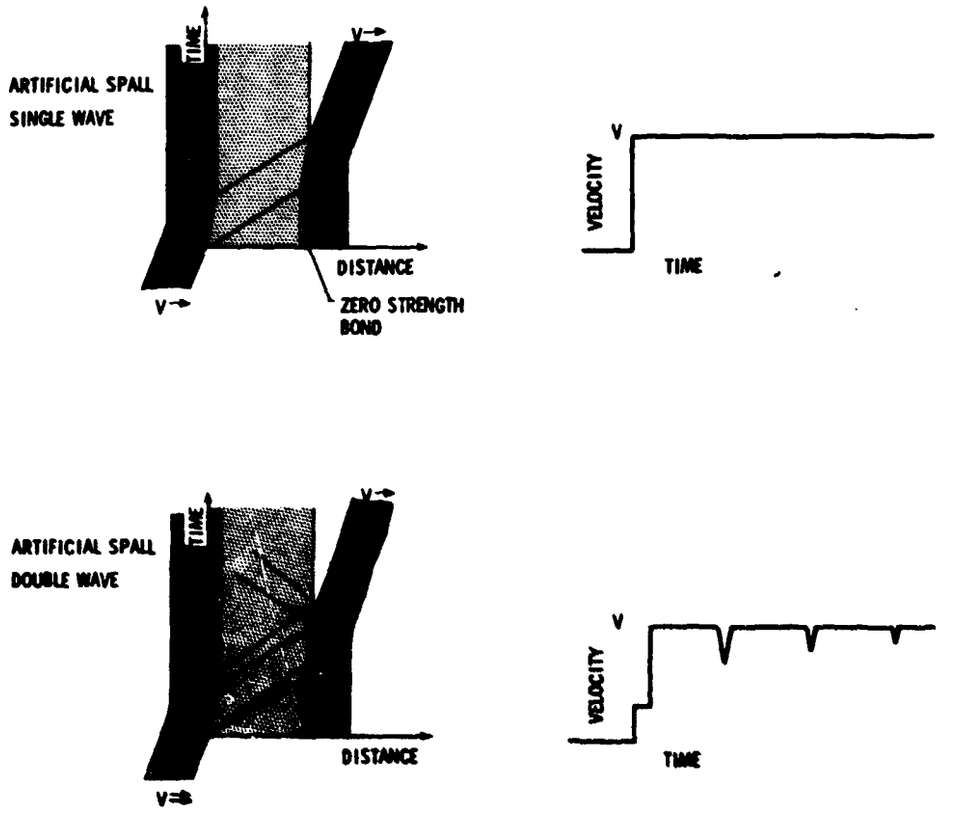

Figure 19 Predicted Wave Profiles from Specimen with Artifical Spall Surface

impactor is simply transferred to the spall piece. For a two-wave system, the momentum transfer will again take place. However, the interactions at the interface are now more complicated and a net tensile stress may develop in the spall piece. The pullback at the rear surface shows evidence of this tensile pulse. Figure 20 shows the measured wave profile for such a test. The ringing in the spall piece continues for many microseconds. The damped pullback apparently will decrease to zero amplitude and the piece will continue with approximately impact velocity.

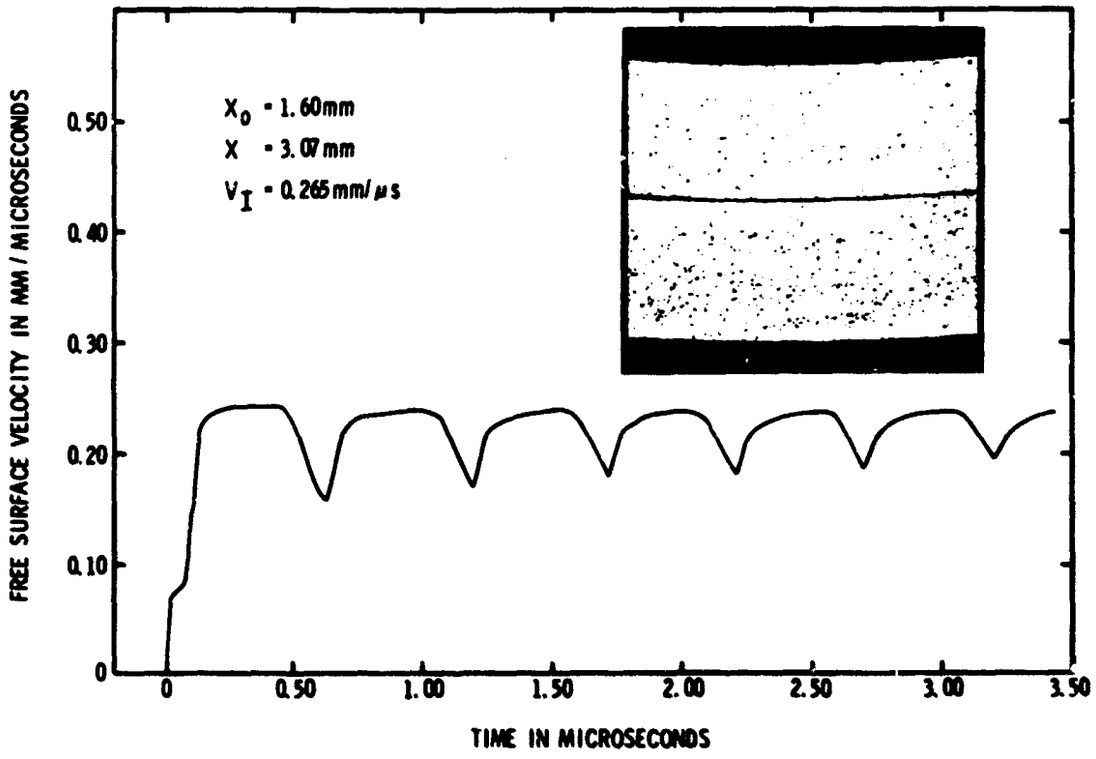

Figure 20 Measured Wave Profile for Artifical Spall

The effect of elevated temperature on profiles of shock waves in 6061-T6 aluminum was studied in the series of tests shown in Figure 21. The tests were conducted using room temperature impactors to induce waves in specimens heated to the test temperature in approximately 10 minutes. The wave profiles have been normalized at several places to facilities various comparisons. In particular, the profiles have been made to agree at (1) the arrivals of the elastic waves, (2) the maximum free surface velocities, and (3) the arrivals of the elastic release waves. The amplitude of the elastic precursor decreases with temperature. The plastic wave velocity decreases with increasing temperature and it takes longer for

MSL-69-60

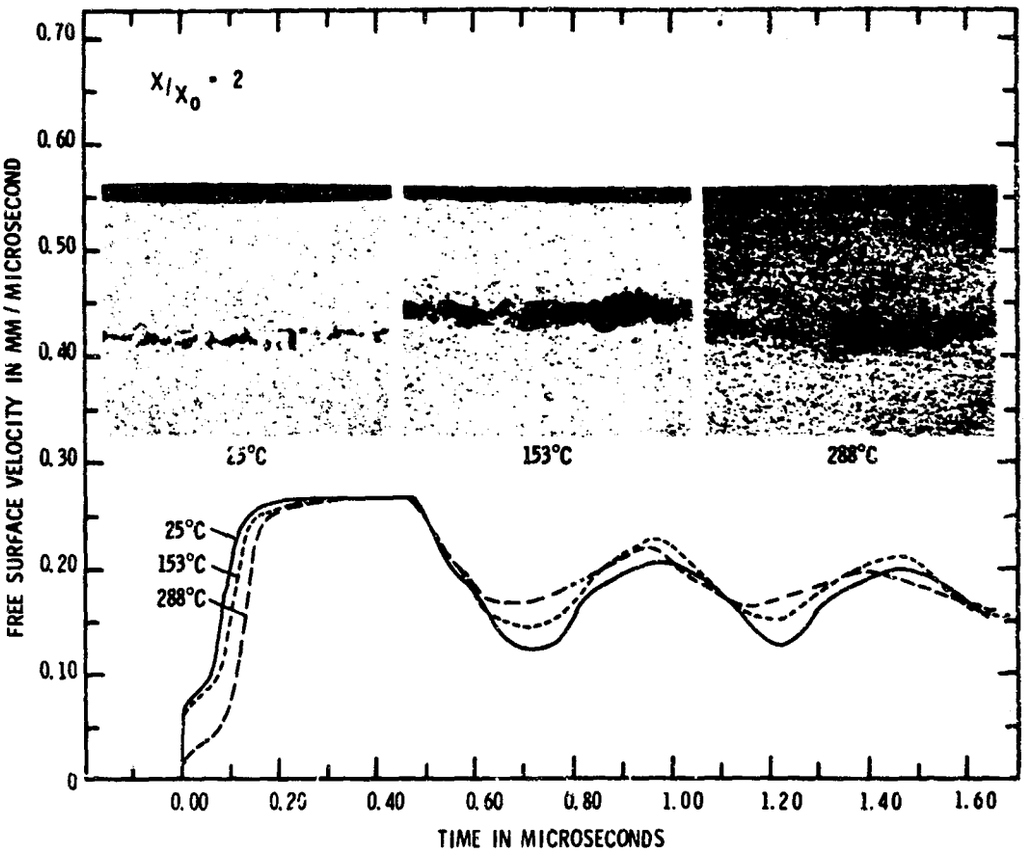

Figure 21 Qualitative Behavior of Aluminum Profiles at Elevated Temperatures

the free surface velocity to reach constant level. The amplitudes of the elastic release waves do not appear proportional to the elastic precursors. Two factors may contribute to this. (1) There is an impedance mismatch and a difference in the value of the elastic limit between the 25°C impactor and the heated target. (2) The heated specimen may be able to sustain a higher amplitude elastic wave in rarefaction than it can in compression due to work-hardening of the material during the compression phase. The relative pullbacks of the three profiles show decreasing amplitude with

increasing temperature. Applying Equation 1, where ρ and C are now functions of temperature, the maximum tensile stress at the spall plane decreases from 12 kbars at 25°C to 8 kbars at 288°C.

The most common use of the flat plate technique utilizes target/impactor thickness ratios of two to four and gives quasi-rectangular stress pulses at the spall plane. This approach permits determination of spall fracture characteristics for well-defined stress pulses but does not provide a very stringent check on models of spall fracture or computer codes developed to predict wave propagation and fracture. The ability to adjust the shape of the shock wave causing spallation is useful in evaluating different models and codes. Three waveforms of substantially different shapes that can be generated with flat plate techniques are shown in Figure 22. (1) The rectangular waveshape is characterized by relatively steep compressive and release portions, with a steady-state plateau of time duration determined primarily by the impactor thickness. (2) The release gradient waveshape is achieved for large propagation distances where the release wave has overtaken and partially attenuated the shock front, giving a steep compressive portion with a more gradual release and essentially no steady-state plateau. (3) The compressive gradient waveshape is obtained by using a fused quartz buffer plate between the impactor and the target, giving a gradual compressive gradient followed by steep release. This unusual behavior is a result of the concave downward shape of the fused quartz hugoniot in the stress-particle velocity plane (<30 kbars), which tends to spread the compressive wave, while the release wave has a tendency to shock-up.

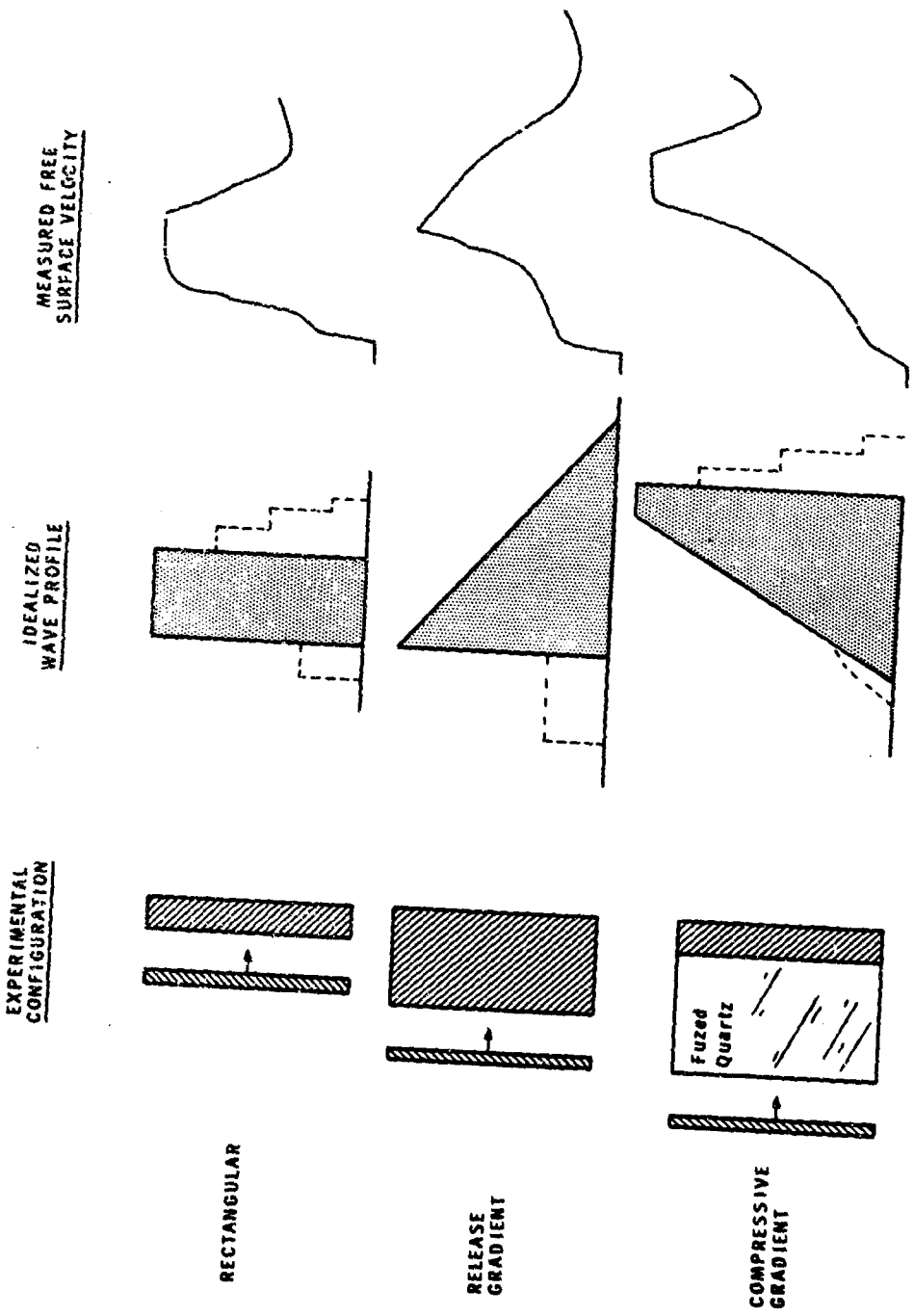

Figure 22 Three Waveshapes for Spall Studies

SUMMARY

Spall fracture in 6061-T6 aluminum as a result of shock wave loading is of a ductile nature, characterized by the coalescence of voids to form elongated cracks in and about the nominal spall plane. The complex, time-dependent fracture process occuring at the spall plane is communicated to the rear surface of the specimen and affects the velocity-time history of the surface. Measurements of the wave profile at this surface can be utilized to furnish quantitative data on the fracture developing within the specimen. An estimate of the maximum stress at the spall plane can be obtained from the simple relation, $\sigma_t = \rho C(\Delta V/2)$ where ΔV is the "pullback" in rear surface velocity due to spall fracture. For the conditions studied, the rear surface pullback was found to be influenced by pulse shape and material temperature, but relatively insensitive to initial impact stress or degree of final fracture. Examination of the rear surface velocity-time profile may also provide data on the time dependence of fracture and on wave damping characteristics. Analysis is complicated, however, by such factors as uncertainty in the negative stress equation of state, incomplete understanding of the spall fracture mechanisms, and three-dimensional effects in the vicinity of the spall fractures. Various experimental techniques can be used to adjust wave forms and corresponding stress gradients, permitting a more stringent evaluation of models and computer codes used to predict wave propagation and dynamic fracture.

REFERENCES

1. "Materials Data Handbook, Aluminum Alloy 6061", NASA Office of Technology Utilization, TSP 69-10065, 1969 (PB 183426).

2. Munson, D. E. and Barker, L. M., "Dynamically Determined Pressure-Volume Relationships for Aluminum, Copper, and Lead", J. Appl. Phys., Vol. 37, 15 March, 1966, pp. 1652-1660.

3. Anderson, O. L., "The Use of Ultrasonic Measurements Under Modest Pressure to Estimate Compression at High Pressure", J. Phys. Chem. Solids, Vol. 27, 1966, pp. 547-565.

4. Babcock, S. G., Kumar, A., and Green, S. J., "Response of Materials to Suddenly Applied Stress Load", GM Defense Research Laboratories, Santa Barbara, California, AFFDL-TR-67-35, Part I, April, 1967.

5. Tuler, F. R., "Fracture Surface Observations in 6061-T6 Aluminum at Different Strain Rates", Sandia Laboratories, Albuquerque, New Mexico, SC-DR-68-497, October, 1968.

6. Beacham, C. D., "An Electron Fractographic Study of the Influence of Plastic Strain Conditions Upon Ductile Rupture Processes in Metals", ASM Trans., Vol. 56, Sept., 1963, pp. 318-326.

7. Karnes, C. H., "The Plate Impact Configuration for Determining Mechanical Properties of Materials at High Strain Rates", Mechanical Behavior of Materials Under Dynamic Loads, Springer-Verlag New York Inc., 1968, pp. 270-293.

8. Preonas, D. D., "AFML Electrical Plate Slap Facility", Air Force Materials Laboratory, Wright-Patterson AFB, Ohio, AFML-TR-68-352, November, 1968, (AD 685 189).

9. Breed, B. R., Mader, C. L., and Venable, D., "Technique for the Determination of Dynamic-Tensile-Strength Characteristics", J. Appl. Phys., Vol. 38, No. 8, July, 1967, pp. 3271-3275.

10. Graham, R. A. and Hutchinson, R. E., "Thermoelastic Stress Pulses Resulting from Pulsed Electron Beams", Appl. Phys. Letters, Vol. 11, No. 2, 15 July, 1967, pp. 67-71.

11. Miller, D. R., "Ductile Fracture", J. Aust. Inst. Metals, Vol. 14, No. 1, February, 1969, pp. 38-41.

12. Smith, J. H., "Three Low-Pressure Spall Thresholds in Copper", Dynamic Behavior of Materials, American Society for Testing Materials, Philadelphia, 1963, pp. 264-282.

13. Butcher, B. M., Barker, L. M., Munson, D. E., and Lundergan, C. D., "Influence of Stress History on Time-Dependent Spalls in Metals", AIAA J., Vol. 2, No. 6, June, 1964, pp. 977-990.

14. Oscarson, J. H. and Graff, K. F., "Spall Fracture and Dynamic Response of Materials", Battelle Memorial Institute, Columbus, Ohio, BAT-197A-4-3, 21 March, 1968 (AD 669 440).

15. Thurston, R. S. and Mudd, W. L., "Spallation Criteria for Numberical Calculations", Los Alamos Scientific Laboratory, New Mexico, LA-4013, Sept., 1968.

16. Tuler, F. R. and Butcher, B. M., "A Criterion for the Time Dependence of Dynamic Fracture", Int. J. Fracture Mechanics, Vol. 4, No. 4, December, 1968, pp. 431-437.

17. Taylor, J. W., "Stress Wave Profiles in Several Metals", Dislocation Dynamics, McGraw-Hill, New York, 1968, pp. 573-589.

18. Barker, L. M., "Fine Structure of Compressive and Release Wave Shapes in Aluminum Measured by the Velocity Interferometer Technique", Behavior of Dense Media Under High Dynamic Pressures, Gordon and Breach, New York, 1968, pp. 483-505.

19. Mader, C., Los Alamos Scientific Laboratory, Private Communication.

UNCLASSIFIED
Security Classification

DOCUMENT CONTROL DATA - R & D

(Security classification of title, body of abstract and indexing annotation must be entered when the overall report is classified)

1. ORIGINATING ACTIVITY (Corporate author)	2a. REPORT SECURITY CLASSIFICATION
Manufacturing Dev., General Motors Corporation, G. M. Technical Center, Warren, Michigan 48090	UNCLASSIFIED
	2b. GROUP

3. REPORT TITLE

SHOCK PROPAGATION AND FRACTURE IN 6061-T6 ALUMINUM FROM WAVE PROFILE MEASUREMENTS

4. DESCRIPTIVE NOTES (Type of report and inclusive dates)

Interim Technical Report

5. AUTHOR(S) (First name, middle initial, last name)

William M. Isbell, Douglas R. Christman

6. REPORT DATE	7a. TOTAL NO. OF PAGES	7b. NO. OF REFS
1970, April	38	19

8a. CONTRACT OR GRANT NO.	9a. ORIGINATOR'S REPORT NUMBER(S)
DASA-01-68-C-0114	Manufacturing Development General Motors Corporation Report MSL-69-60
b. PROJECT NO. NWER Subtask AA 106	
c. Work Unit 07	9b. OTHER REPORT NO(S) (Any other numbers that may be assigned this report)
d.	DASA 2419

10. DISTRIBUTION STATEMENT

This document has been Approved for Public Release and Sale: Its Distribution is Unlimited.

11. SUPPLEMENTARY NOTES	12. SPONSORING MILITARY ACTIVITY
	Director Defense Atomic Support Agency Washington, D. C. 20305

13. ABSTRACT

The use of high-resolution, time-resolved measurements of rear surface velocity in shock loaded 6061-T6 aluminum is discussed as a means of studying spall fracture. The influence of stress pulse shape, material temperature, maximum compressive stress and degree of fracture on free surface motion is presented and correlated with maximum tensile stress at the spall plane. A summary of dynamic properties data (equation of state, elastic wave velocity, stress-strain-strain rate behavior, spall threshold) and a brief discussion on fracture in metals are also given.

DD FORM 1 NOV 65 1473

UNCLASSIFIED
Security Classification